HHS Public Access

Author manuscript

Clin Cancer Res. Author manuscript; available in PMC 2019 May 15.

Published in final edited form as:

Clin Cancer Res. 2018 May 15; 24(10): 2370–2382. doi:10.1158/1078-0432.CCR-17-2545.

Chemotherapy induces breast cancer stemness in association with dysregulated monocytosis

Liang Liu[2], **Lin Yang**[3], **Wei Yan**[1], **Jing Zhai**[4], **Donald P. Pizzo**[1], **Peiguo Chu**[5], **Andrew R. Chin**[1], **Meng Shen**[2], **Chuan Dong**[1], **Xianhui Ruan**[6], **Xiubao Ren**[2,*], **George Somlo**[7,*], and **Shizhen Emily Wang**[1,2,*]

[1]Department of Pathology, University of California, San Diego; La Jolla, California, 92093, USA

[2]Department of Immunology and Biotherapy, Tianjin Medical University Cancer Institute and Hospital; Tianjin, 300060, China

[3]Institute of Hematology and Blood Diseases Hospital, Chinese Academy of Medical Sciences and Peking Union Medical College; Tianjin, 300020, China

[4]Department of Pathology & Laboratory Medicine, Cedars-Sinai Medical Center; Los Angeles, California, 90048, USA

[5]Department of Pathology, City of Hope National Medical Center and Comprehensive Cancer Center; Duarte, California, 91010, USA

[6]Department of Thyroid and Neck Tumor, Tianjin Medical University Cancer Institute and Hospital; Tianjin, 300060, China

[7]Department of Medical Oncology, City of Hope National Medical Center and Comprehensive Cancer Center; Duarte, California, 91010, USA

Abstract

Purpose—Preoperative or neoadjuvant therapy (NT) is increasingly used in patients with locally advanced or inflammatory breast cancer (BC) to allow optimal surgery and aim for pathological response. However, many BCs are resistant or relapse after treatment. Here, we investigated conjunctive chemotherapy-triggered events occurring systemically and locally, potentially promoting a cancer stem-like cell (CSC) phenotype and contributing to tumor relapse.

Experimental Design—We started by comparing the effect of paired pre- and post-NT patient sera on the CSC properties of BC cells. Using cell lines, patient-derived xenograft models and primary tumors, we investigated the regulation of CSCs and tumor progression by chemotherapy-induced factors.

Correspondence address: Shizhen Emily Wang (emilywang@ucsd.edu), Department of Pathology, University of California, San Diego, 9500 Gilman Drive, MC 0612, La Jolla, CA 92093, USA, Tel: +1 858-2462464.

*Co-senior authors

Author contributions

S.E.W. and G.S. conceived ideas, and X.Ren and L.L. contributed to project planning. L.L., L.Y., and S.E.W. designed and performed most of the experiments. W.Y., A.R.C., M.S., C.D., and X.Ruan assisted with the Western analyses and ELISA. D.P.P., J.Z., and P.C. performed IHC staining and pathological evaluation. S.E.W., G.S., and X.Ren wrote the manuscript.

Conflict of interest: Genentech and Celgene advisory board and grant support to institution (G.S.).

Results—In human patients and mice, we detected a therapy-induced CSC-stimulatory activity in serum, which was attributed to therapy-associated monocytosis leading to systemic elevation of monocyte chemoattractant proteins (MCPs). The post-NT hematopoietic regeneration in the bone marrow highlighted both altered monocyte-macrophage differentiation and biased commitment of stimulated hematopoietic stem cells towards monocytosis. Chemotherapeutic agents also induce monocyte expression of MCPs through a JNK-dependent mechanism. Genetic and pharmacological inhibitions of the MCP-CCR2 pathway blocked chemotherapy's adverse effect on CSCs. Levels of nuclear Notch and ALDH1 were significantly elevated in primary BCs following NT, whereas higher levels of CCR2 in pre-NT tumors were associated with a poor response to NT.

Conclusions—Our data establish a mechanism of chemotherapy-induced cancer stemness by linking the cellular events in the bone marrow and tumors, and suggest pharmacological inhibition of CCR2 as a potential co-treatment during conventional chemotherapy in neoadjuvant and adjuvant settings.

Keywords

Chemotherapy; Cancer stem-like cells; Breast cancer; Monocyte chemoattractant proteins; CCR2

Introduction

Cytotoxic chemotherapy is used as conventional treatment for cancer in adjuvant and neoadjuvant settings and as induction therapy in *de novo* stage IV breast cancer (BC). The cancer cell population is influenced directly by the therapeutic agents and indirectly by therapy-associated changes that occur in the tumor microenvironment and possibly also at the systemic level. Compared to adjuvant chemotherapy aiming to target residual cancer cells upon surgical removal of a majority of the tumor mass, neoadjuvant therapy (NT) exerts direct and indirect effects on the entire population of cancer cells that present preoperatively. The promise of NT relies on the potentials to downstage tumors thus allowing optimal surgery, to eradicate clinically undetectable disseminated cancer cells, and to test the efficacy of therapy. In BC and several major human cancers, NT has been shown to significantly improve clinical parameters and outcomes (1–3).

In the treatment of BC, NT is increasingly administered to candidates for breast preservation and/or present with locally advanced or inflammatory BC. Although only 10–30% of treated hormone receptor-positive (HR^+) BC patients exhibit pathologic complete response (pCR) in breast and in regional lymph nodes, the pCR rate of BCs characterized as triple negative (TN) or $HER2^+$ untreated BCs is over 50% (4,5). Evidence is emerging about the association between pCR and long-term progression-free and overall survival, particularly in HR^- BCs. However, after NT, some patients with pCR and more with non-pCR relapse, or progress (in the case of non-pCR) with stage IV metastatic BC, which is ultimately fatal (6). Therefore, understanding both *de novo* and acquired resistance to NT or induction therapy is of utmost importance. Mechanisms of BC resistance are partly intrinsic to cancer cells, including altered drug metabolism and enhanced damage repair and survival capacities (7). More recently, the complex role of the tumor microenvironment has become clearer; cytokines and other secreted factors produced by stromal fibroblasts, endothelial cells, and certain tumor-

infiltrating immune cells have been shown to impede the tumor response to conventional and targeted therapies (8,9). In addition, accumulating evidence indicate the critical role of a cancer stem-like cell (CSC) phenotype in resistance to therapy.

CSCs are defined as a subset of cancer cells that can proliferate/maintain/differentiate into a new phenotypically heterogeneous tumor, resembling normal stem cells in the self-renewing and pluripotent capacities and undifferentiated gene expression patterns (10,11). CSCs are implicated in tumor initiation (as the tumor-initiating cells), sustained tumor growth (by undergoing self-renewal and generating cells with diverging phenotypes), therapy refractoriness (by expressing drug transporters and remaining dormant in the tumor), and metastasis (as seeds for distant colonization) (12). A variety of cell surface markers and phenotypic markers have been used to enrich CSCs from bulk tumor cells; for human BC, these include $CD44^{+}/CD24^{-/low}$, expression or activity of aldehyde dehydrogenase 1 (ALDH1), and the ability to escape anoikis and grow into spheres in anchorage-independent conditions (10,13,14). The diverse and dynamic nature of CSCs has been recognized: the gene expression markers of CSCs may vary between tumors and multiple CSC pools may exist within individual tumors; CSCs may undergo genetic evolution during cancer recurrence and metastasis; and non-stem cancer cells may reversibly switch to CSCs (12). Therefore, effective therapies against cancer stemness need to target all CSC subsets existing in the tumor and meanwhile block new CSC emergence, such as those potentially induced by therapy.

Several studies have reported that post-NT breast tumors exhibit a higher CSC frequency (15) and stemness-associated gene expression (16). However, it remains unclear if the CSC population, in addition to escaping the cytotoxic effect of NT, also undergo therapy-induced expansion. We therefore set out to determine if and how NT impacts on the CSC traits, to shed light on selecting patients who may benefit from potential combination therapy targeting NT-induced cancer stemness.

Materials and Methods

Clinical specimens

Human specimens were obtained from voluntarily consenting BC patients at the City of Hope National Medical Center (Duarte, CA; for Figures 1, 5A, 5C–E, Table 1, and Supplemental Figure 1), or at the Tianjin Medical University Cancer Institute and Hospital (Tianjin, China; for Figure 5B) under institutional review board-approved protocols. Written informed consents were obtained from all patients. The studies were conducted in accordance with recognized ethical guidelines. Patients from the City of Hope were participants of clinical trials NCT01525966, NCT01730833, or NCT00295893 (ClinicalTrials.gov Identifier). Clinical information, including age, tumor stage and pathology, as well as NT starting time, regimen, and response, is summarized in Supplemental Table 1.

Cells and constructs

BC cell lines MDA-MB-231, BT474, and 4T1 as well as the monocytic cell line THP-1 were obtained from American Type Culture Collection (Manassas, VA) and cultured in DMEM (for MDA-MB-231) or RPMI-1640 (for BT474, 4T1, and THP-1) base medium supplemented with 10% fetal bovine serum (FBS). The patient-derived PDX265922 cells originating from a triple-negative breast tumor and propagated in NSG mice as well as the primary cancer-associated fibroblasts (CAF) from the same human tumor are described previously (17). All cells used herein were tested to be free of mycoplasma contamination and authenticated by using the short tandem repeat profiling method at the beginning and end of the study. Aliquots of frozen cell stocks were prepared immediately, and used to replace cells in culture every two months. Lentiviral constructs expressing shRNAs against CCR1-3 as well as a scrambled control were purchased from GeneCopoeia (Rockville, MD) to generated MDA-MB-231 cells with stable gene knockdown (CCR1: #HSH002198-LVRU6MP; CCR2: #HSH002200-LVRU6MP; CCR3: #HSH002207-LVRU6MP; control: #CSHCTR001-LVRU6MP). For CCR1-3, each set contains 4 shRNA expression constructs coded as #1–4. Production of viruses, infection, and selection of transduced cells were carried out as previously described (17). The two shRNA constructs showing greatest gene knockdown efficiency were shown in Supplemental Figure 3A–C. Recombinant human CCL2, CCL7, and CCL8, as well as the neutralizing antibodies against human CCL2/7/8 and the control goat IgG were purchased from R&D Systems (Minneapolis, MN). The CCR2 inhibitor MK-0812 was purchased from Cayman Chemical (Ann Arbor, MI). Doxorubicin, docetaxel, and SP600125 were purchased from Sigma-Aldrich (St. Louis, MO). RO4929097 was purchased from Selleckchem (Houston, TX).

Cytokine array and ELISA

Paired pre- and post-NT human sera were analyzed for changes in cytokine levels by using RayBio C-series human cytokine antibody array C3 (RayBiotech; Norcross, GA) following the manufacturer’s protocol. Levels of MCPs in human and mouse sera were measured by the corresponding ELISA kits. The human CCL2/7/8 and the mouse CCL2/8 DuoSet ELISA kits were purchased from R&D Systems. The CCL7 mouse ELISA kit was purchased from Cusabio (College Park, MD).

Co-culture assay

Monocytes used in co-culture assays were isolated by EasySep mouse monocyte isolation kit (Stemcell Technologies; Vancouver, BC, Canada) from the peripheral blood of C57BL/6 mice after 4 weekly treatments with doxorubicin (4 mg/kg), docetaxel (25 mg/kg), or PBS. THP-1 cells were pre-treated with doxorubicin (125 nM), docetaxel (4 nM), or PBS for 48 h. The co-culture was set up in RPMI-1640 medium supplemented with 10% FBS by seeding BC cells in the lower chamber and mouse or human monocytes in the upper chamber of a 0.4-μm transwell insert (Corning; Corning, NY). After 48 h, cancer cells were harvested for analyses.

Flow cytometry and cell sorting

Single-cell suspensions prepared from cell culture or tissue were analyzed by ALDEFLUOR assay kit (#01700; Stemcell Technologies) following the manufacturer's protocol. Flow cytometry was performed using a CyAn ADP flow cytometer (Dako; Carpinteria, CA) and analyzed by FlowJo software (TreeStar; Ashland, OR). Cell sorting based on intensity of ALDEFLUOR was performed using a FACSAria III cell sorter (BD Biosciences; San Jose, CA). Antibodies used for stemness analysis are: APC anti-human CD326 (EpCAM/ESA) (#324208; BioLegend, San Diego, CA); FITC anti-human CD44 (#555478; BD Biosciences); PE anti-human CD24 (#555428; BD Biosciences). For the flow cytometry of bone marrow (BM) hematopoietic cells, femora and tibiae were collected from C57BL/6 mice at the indicated time points, and BM cells were flushed with MACS buffer and analyzed as described (18). To characterize the hematopoietic progenitors, cells were negatively selected for Lin (Ter119-APC-eFluor 780, #47-5921-82; Gr1-APC-eFluor 780, #47-5931-82; B220-APC-eFluor 780, #47-0452-82; CD3e-APC-eFluor 780, #47-0031-82; CD11b-APC-eFluor 780, #47-0112-82; CD4-APC-eFluor 780, #47-0041-82; CD8a-APC-eFluor 780, #47-0081-82) (eBioscience; San Diego, CA), and stained with c-Kit-APC (#17-1171-81), Sca-1-PE-Cy7 (#25-5981-81), CD34-FITC (#11-0341-81), and CD16/CD32-PE (FcgR-III/II) (#12-0161-81) antibodies (eBioscience) for 30 min before analyzed by a BD FACSCanto II flow cytometer and BD FACSDiva software (BD Biosciences). Macrophage and monocyte characterization did not include the Lin negative selection, and cells were stained with CD3-Alexa Fluor 700 (#561388), B220-Alexa Fluor 700 (#557957) (BD Biosciences), NK1.1-FITC (#11-5941-81), CD115-APC (#17-1152-82), and F4/80-PE (#12-4801-82) (eBioscience) antibodies. The cell populations were identified as: HSC, Lin$^-$c-Kit$^+$Sca-1$^+$; CMP, Lin$^-$c-Kit$^+$Sca-1$^-$CD16/CD32^{low}CD34$^+$; GMP, Lin$^-$c-Kit$^+$Sca-1$^-$CD16/CD32^{high}CD34$^+$; MEP, Lin$^-$c-Kit$^+$Sca-1$^-$CD16/CD32$^-$CD34$^-$; macrophages, CD3$^-$B220$^-$NK1.1$^-$F4/80$^+$CD115$^-$, Low SSC; monocytes, CD3$^-$B220$^-$NK1.1$^-$F4/80$^-$CD115$^+$. Complete blood count was performed using a Sysmex XT-2000i hematology analyzer (Sysmex Corporation; Kobe, Japan).

Sphere formation assay

Mammosphere culture was performed as previously described (17). Cells pre-treated with MCPs for 48 h were seeded in ultralow attachment 6-well plates (Corning; Corning, NY). The number of spheres (diameter ≥ 70 μm) was counted on day 10, and sphere forming efficiency was calculated based on the number of initially seeded cells.

RNA extraction and quantitative reverse transcription PCR

These procedures were performed as described previously (17). Primers used are indicated in Supplemental Table 2. An annealing temperature of 55°C was used for all primers.

Western blot analysis

These procedures were performed as described previously (19). Protein extracts were separated by electrophoresis on a 10% or 12% SDS polyacrylamide gel. Protein detection was performed using the following antibodies: NICD (#4147; Cell Signaling Technology);

SOX9 (#AB5535; EMD Millipore, Billerica, MA); NANOG (#3580; Cell Signaling Technology); and GAPDH (#2118; Cell Signaling Technology).

IHC

IHC staining of formaldehyde-fixed, paraffin-embedded tumor tissues was performed as previously reported (17) using the following antibodies and dilutions: Ki-67 (#M7240; Dako, Carpinteria, CA), 1:50 dilution; NOTCH1 (#ab52627; Abcam), 1:35 dilution; ALDH1 (#611194; BD Biosciences), 1:100 dilution; and CCR2 (#ab176390; Abcam), 1:3000 dilution. Stained slides were scored according to intensity of staining (-: 0; +: 1; ++: 2; and +++: 3) and percentage of tumor cells staining positive for each antigen (0%: 0; 1~29%: 1; 30~69%: 2; and ≥ 70%: 3). The intensity score was multiplied by the percentage score to obtain a final score, which was used in the statistical analyses.

Animals

All animal experiments were approved by the institutional animal care and use committee at the University of California San Diego or the City of Hope Beckman Research Institute. Six-week-old female NOD/SCID/IL2Rγ-null (NSG), BALB/c, or C57BL/6 mice were used. For the mouse serum analyses in Figure 1E–G, tumor-free NSG mice and those with MDA-MB-231 xenograft tumors of ~200 mm^3 in the No. 4 mammary fat pad, as well as tumor-free BALB/c mice received 3 weekly intraperitoneal (i.p.) injections with doxorubicin (4 mg/kg), docetaxel (25 mg/kg), or PBS as control. Serum was collected 6 days after the last injection. For the limiting-dilution transplantation in Figure 1H, MDA-MB-231 cells pre-treated with human serum (case T1) or mouse serum (pooled from 5 tumor-free BALB/c mice) for 48 h were injected into the mammary fat pads of NSG mice at the indicated numbers. Tumor incidence after 4 weeks was shown. The tumor-initiating cell (TIC) frequency was estimated by extreme limiting dilution analysis (ELDA) (20). For the monocyte depletion experiments in Figure 2A–C, clodronate liposome or control (Liposoma B.V., Amsterdam, the Netherlands; 200 μL for the first treatment and 100 μL thereafter) were injected into BALB/c mice through the tail vein every 2 days starting at 2 days prior to the first chemotherapy treatment. At day 6 after 3 weeks of chemotherapy, blood and BM were collected. For the complete blood count analyses in Figure 2D and Supplemental Figure 2, BALB/c and C57BL/6 mice received 4 times of treatment with doxorubicin, docetaxel, or PBS, on days 1, 7, 14, and 21. Blood was collected via the tail vein at each indicated time point. For the bulk cancer cell transplantation in Figure 4A–C, 10^6 MDA-MB-231 cells with stable knockdown of CCR2 (shCCR2 #1) or those expressing control shRNA (shCTRL) were injected into the #4 mammary fat pad of NSG mice. When tumor size reached ~250 mm^3, mice were treated weekly with docetaxel for 3 weeks, and then left free of chemotherapy until the end of experiment. One group with MDA-MB-231-shCTRL tumors also received the CCR2 inhibitor MK-0812 (oral 30 mg/kg twice a day) starting with the chemotherapy and continuing for a total of 30 days. For the $ALDEFLUOR^{bright}$ cancer cell transplantation in Figure 4D–J, BALB/c and NSG mice were treated with doxorubicin, docetaxel, or PBS for 3 weeks and then left free of chemotherapy for 1 week, before 10^3 freshly sorted $ALDEFLUOR^{bright}$ 4T1 or PDX265922 cells were injected into the #4 mammary fat pad to assess tumor development. As indicated, some mice received oral MK-0812 or vehicle twice a day at 30 mg/kg starting with the chemotherapy and continuing

for 30 days after BC cell engraftment. Tumor volume was determined by caliper measurements.

Statistics

All quantitative data are presented as mean ± standard deviation (s.d.). Two-sample two-tailed Student t-tests were used for comparison of means of quantitative data between two groups. For multiple independent groups, one-way ANOVA with post-hoc Tukey tests were used. Nonparametric Wilcoxon tests were used for comparison of paired pre- and post-NT patient samples. Nonparametric Mann–Whitney U tests were used for comparison between two independent patient groups. Values of $P<0.05$ were considered significant. Sample size was generally chosen based on preliminary data indicating the variance within each group and the differences between groups. For animal studies, sample size was predetermined to allow an 80% power to detect a difference of 50%. Animals were randomized before treatments. For experiments in which no quantification is shown, images representative of at least three independent experiments are shown.

Data and materials availability

All materials, data, and protocols described in the manuscript are available from the corresponding author on reasonable request.

Results

Post-chemotherapy sera stimulate a CSC phenotype through elevated MCP levels

To determine if systemic factors (e.g., cytokines), altered by anticancer therapies, may regulate the CSC phenotype, we first compared the effects of paired pre- and post-treatment sera from TN and $HER2^+$ BC patients who had received NT. TNBC patients received carboplatin and a taxane and those with $HER2^+$ BCs received these agents plus a HER2-targeting therapy. Patient serum was added to MDA-MB-231 TNBC cells or BT474 $HER2^+$ BC cells at 10% to replace the FBS in regular medium. In both BC models, the post-NT serum significantly induced cell populations that are enriched for BCSCs [the $ALDEFLUOR^{bright}$ population in MDA-MB-231 and the $ESA^+CD44^+CD24^{-/low}$ population in BT474 (10,14)] compared to paired pre-NT serum (Figure 1A; Supplemental Figure 1A). Using a semi-quantitative cytokine array, we detected elevated levels of CCL2 (MCP-1), CCL7 (MCP-3), and CCL8 (MCP-2) in post-NT sera (Supplemental Figure 1B). This was confirmed by ELISA (Figure 1B). When cases were stratified by BC's response to NT or by HER2 status, the blood-borne CSC-stimulating activity as well as levels of all three MCPs were significantly induced following NT in both pCR and non-pCR groups, and in both TNBC and $HER2^+$ groups (Table 1), indicating these NT-associated effects occur regardless of tumor response and HER2 status. Antibody-mediated neutralization of MCPs, especially CCL2, or inhibition of the MCP receptor CCR2 that serves as a major receptor for all three MCPs using its antagonist MK-0812 (21), impaired or abolished the ability of post-NT sera to induce CSCs (Figure 1C, 1D; Supplemental Figure 1C). Therefore, MCP signaling through CCR2 plays an essential role in mediating the CSC-inducing activity in post-NT human blood.

We next examined if chemotherapy led to a similar result in mouse serum, and if the presence of a tumor is required for this therapy-induced effect. Female NSG mice with or without MDA-MB-231 orthotopic xenograft tumors, as well as tumor-free BALB/c mice, received three weeks of doxorubicin or docetaxel treatment before the serum was collected and added to MDA-MB-231 cells *in vitro* for evaluation of CSC markers. The results indicate that, similar to humans, mice induce a tumor-independent blood-borne activity after chemotherapy that expands ALDEFLUOR^{bright} BC cells, and that MCPs as well as their receptor CCR2 also mediate this effect in both immuno-competent and -compromised mice (Figure 1E–1G). Importantly, when varying numbers of MDA-MB-231 cells pre-treated with pre-/post-NT patient sera, or with pre-/post-docetaxel sera from tumor-free NSG mice, were injected into the mammary fat pad of NSG mice in a limiting-dilution transplantation assay, post-chemotherapy sera from both human and mice exhibited enhanced ability to stimulate tumorigenicity (Figure 1H). Therefore, the post-therapy serum activity to contain elevated MCP levels and stimulate CSCs is consistently observed in mice and humans, and does not require tumor cells or cells in the tumor microenvironment.

Chemotherapy-induced monocytosis is responsible for the elevation of circulating MCPs

To determine if therapy-induced MCPs are mainly produced by monocytes, we treated BALB/c mice intravenously with the monocyte-depleting agent clodronate prior to and during chemotherapy treatment. Mice receiving clodronate showed lower basal levels of monocytes and a complete blockade of monocyte induction following chemotherapy compared to the control group, which showed monocyte induction in the blood and BM following drug treatments (Figure 2A). The clodronate-treated mice also failed to exhibit chemotherapy-induced MCP release (Figure 2B) and CSC-stimulating activity in the blood (Figure 2C). In the BALB/c model, total white blood cells (WBCs) showed a ~40–60% decrease after 2–3 times of treatment with doxorubicin or docetaxel. This was followed by a rapid restoration of WBCs to levels near or slightly above the pre-treatment baseline. The dynamics of WBCs parallels lymphocyte response to treatment (Figure 2D). In contrast, the blood monocyte population significantly expanded during the rebound phase, and remained higher than the baseline for more than 20 days after the last drug treatment (Figure 2D). Similar to monocytes, neutrophils also exhibited rebound expansion, whereas the numbers of red blood cells and platelets did not dramatically fluctuate. The leukocyte dynamics in the blood was consistent with the BM cell numbers, suggesting the post-therapy monocyte expansion in the peripheral blood results from BM reconstitution. This post-therapy rebound is not likely to result from injection-associated inflammation, because injections with PBS did not significantly alter WBC or monocyte numbers, and the two tested drugs injected at the same frequency showed differences in the strength and time course of monocyte regulation.

The post-chemotherapy induction of circulating monocytes was also observed in C57BL/6 mice (Supplemental Figure 2). Using established cell surface markers (18), we analyzed the hematopoietic regeneration in the BM of these mice following chemotherapy treatment. Compared to the control group receiving PBS, both doxorubicin and docetaxel induced an expansion of HSCs that began immediately and climaxed after the last treatment. While little effects were observed with the common myeloid progenitors (CMPs), concurrently

increased granulocyte-monocyte progenitor (GMP) and decreased megakaryocyte-erythrocyte progenitor (MEP) populations were detected after 4 times of chemotherapy treatment (Figure 2E, 2F). In addition, we observed a significant shift of the F4/80^{+}CD115^{-} macrophages to F4/80^{-}CD115^{+} monocytes starting after the first treatment and accumulating thereafter. These results suggest the involvement of a series of post-chemotherapy events in the BM, including the immediately altered monocyte-macrophage differentiation as well as the stimulation of HSC expansion and their biased lineage commitment to generate more GMPs vs. MEPs in a relatively later phase for sustained monocytosis.

Chemotherapy induces monocyte expression of MCPs, which promote the stemness-associated properties by inducing Notch

We next co-cultured BC cells with mouse monocytes isolated pre- and post-chemotherapy or with THP-1 human monocytic cells pre-treated with doxorubicin or docetaxel. In a dose-dependent manner, the post-chemotherapy monocytes exhibited an enhanced ability to stimulate the CSC traits in BC cells, which was abolished by CCR2 inhibition (Figure 3A) or MCP neutralization (Figure 3B). We further found that the chemotherapeutic agents induced the secreted levels of MCPs in monocytes but not in CAF (Figure 3C), and that this induction occurred at the RNA level through a JNK-dependent mechanism (Figure 3D), consistent with a previous report showing JNK-mediated upregulation of *CCL2* through c-Jun-binding sites in the gene promoter (22). When MDA-MB-231 cells were individually treated with recombinant MCPs, all three MCPs, especially CCL7, induced dose-dependent increases in mammosphere formation and the population of ALDEFLUOR^{bright} cells (Figure 3E). Similar results were observed with patient-derived PDX265922 TNBC cells (17) (Figure 3F). In BT474 HER2^{+} BC cells, which naturally harbor a high percentage of ALDEFLUOR^{bright} cells (23), MCPs significantly induced mammosphere formation as well as the subset of ESA^{+}CD44^{+}CD24$^{-/low}$ cells that are known to contain enriched CSCs (10) (Figure 3G). In all BC cells tested, MCPs significantly induced the expression of stemness-related genes, including *SOX9* and *NANOG*, at the mRNA and protein levels, and increased the protein levels of the Notch intracellular domain (NICD), indicating activation of Notch signaling (Figure 3H–I). In support of our previously reported mechanism of CCL2 to activate Notch (17), we found that the ability of all three MCPs to induce stemness genes was completely abolished by a γ secretase inhibitor RO4929097 (Figure 3J). These results collectively indicate that chemotherapy induces monocyte expression of MCPs, which promote CSC properties by inducing Notch signaling.

Chemotherapy promotes CSC properties in vivo through MCP-CCR2 signaling

Based on the *in vitro* data, we hypothesized that the MCP-CCR signaling mediates the post-NT CSC induction and tumor progression. To this end we generated MDA-MB-231 cells with individual knockdown of CCR1-3 (shCCR1-3) or those expressing control shRNA (shCTRL). Stable knockdown of CCR2 but not the other two CCRs efficiently blocked the effects of all three MCPs on inducing stemness-related gene expression and mammosphere formation (Supplemental Figure 3A–C). Pharmacological inhibition of CCR2 with MK-0812 also abolished MCP-mediated induction of NICD and stemness-related genes (Supplemental Figure 3D). We therefore focused on CCR2, and injected 10^{6} of MDA-

MB-231 cells with stable expression of shCCR2 or shCTRL into the #4 mammary fat pad of NSG mice. When tumor size reached ~250 mm^3, mice were treated with docetaxel for 3 weeks, and then left free of chemotherapy until the end of experiment (Figure 4A). One group with MDA-MB-231-shCTRL tumors also received the CCR2 inhibitor MK-0812 starting with the chemotherapy and continuing for a total of 30 days. Tumors with CCR2 knockdown grew slower than the control tumors from the beginning, and exhibited significantly suppressed regrowth after the completion of chemotherapy. Treatment with the CCR2 inhibitor also significantly reduced post-therapy tumor regrowth (Figure 4B). The post-therapy tumors with CCR2 knockdown or treated with CCR2 inhibitor also contained a lower content of $ALDEFLUOR^{bright}$ cells, compared to the control tumors (Figure 4C).

We next examined if chemotherapy prior to BC cell engraftment altered the host environment to enhance tumor formation from prospectively enriched CSCs. One thousand of $ALDEFLUOR^{bright}$ 4T1 or PDX265922 cells were injected into the mammary fat pad of BALB/c or NSG mice, respectively, which had previously received three weekly injections of doxorubicin, docetaxel, or PBS (Figure 4D). Mice pre-treated with chemotherapy developed mammary tumors at an earlier time, and presented tumors with larger size, higher content of $ALDEFLUOR^{bright}$ cells, and increased expression of stemness-related genes (Figure 4E–J). These effects were suppressed by co-treatment with the CCR2 inhibitor MK-0812 (Figure 4H–J). Thus, data from mouse tumor models collectively suggest that chemotherapy promotes CSC-mediated tumor growth through MCP-CCR2 signaling, which may be targeted by pharmacological inhibition of CCR2.

Chemotherapy induces monocytosis as well as markers of NOTCH activation and CSCs in BC patients, whereas tumor expression of CCR2 is associated with NT response

Our data this far suggest that the BCSC population may undergo a dramatic expansion in response to NT through a mechanism involving therapy-induced monocytosis and MCP-CCR2 signaling in cancer cells. To seek additional clinical evidence, we performed complete blood count in two independent cohorts of BC patients to determine changes of various cell populations upon NT. Among patients treated at City of Hope, although the WBC, RBC, and platelet counts were significantly decreased after 6–12 weeks of NT, a significant induction of monocyte content was detected (Figure 5A). Among patients treated at the Tianjin Medical University Cancer Hospital, for which blood was examined weekly, we observed significant induction of monocytes during the rebound phase after each time of chemotherapy (Figure 5B). These results, together with the previously described MCP elevation in post-NT blood (Figure 1B), indicate an upstream role of chemotherapy-induced monocytosis in the herein identified CSC regulatory mechanism.

We further analyzed paired pre- and post-NT breast tumors from the City of Hope patients by immunohistochemistry, and detected significantly increased levels of nuclear Notch 1 in the tumor, together with increased percentage of tumor cells expressing the BCSC marker ALDH1, upon NT treatment (Figure 5C, 5D). Unlike in pre-NT tumors where ALDH1 showed a sparse and scattered staining pattern, $ALDH1^+$ cells in post-NT tumors notably existed in patches, possibly suggesting a clonal origin (Figure 5D). When pre-NT tumors were compared for tumor cell expression of CCR2, those exhibiting pCR during the

subsequent NT had significantly lower CCR2 level compared to tumors with non-pCR (Figure 5E), suggesting that CCR2 expression level which sets tumor responsiveness to MCPs could be a factor influencing tumor response to NT.

Discussion

Although conventional chemotherapy has been known to induce cycles of myelosuppression and restoration (24), how the process of therapy-induced myeloid cell homeostasis may influence tumor relapse has not been fully studied. We show that chemotherapy induces monocytosis and the consequent systemic elevation of MCP chemokines, which occurs regardless of tumor response to therapy, the expression status of HER2, or even the presence of a tumor. Compared to the $HER2^+$ cases, the TNBC cases exhibited higher pre- and post-NT levels of CCL2 and CCL8 and a higher post-NT ALDEFLUOR-stimulating activity in the blood (Table 1). This could suggest the involvement of TNBC-derived factors that also influence MCPs. Our data suggest that HSCs display enhanced commitment to the granulocyte-monocyte lineage following chemotherapy (Figure 2). During hematopoietic development and homeostasis, cytokines derived from hematopoietic and stromal cells play critical roles in the fate determination of HSCs. Lineage-specific cytokines, such as granulocyte-colony stimulating factor (G-CSF) and granulocyte/macrophage-colony stimulating factor (GM-CSF) secreted by BM mesenchymal cells, can be induced by tumor necrosis factor α (TNFα) and interleukin (IL)-1α produced at sites of inflammation, leading to stimulation of multiple stages of granulopoiesis (25). Secretion of inflammatory cytokines has been shown in fibroblasts in response to persistent DNA damage (26) and in peripheral blood mononuclear cells in response to apoptosis induction (27). Therefore, cytotoxic therapeutic agents, by damaging hematopoietic and stromal cells in the BM and/or inducing hematopoietic stresses, may alter the local cytokine network to effect the complex cell dynamics in the BM observed in Figure 2E–F.

In addition to enhanced monocytosis, chemotherapy also increases the production of MCPs by monocytes but not CAF, which also secrete MCPs but at lower levels (Figure 3C). This effect is dependent on JNK, a stress-activated protein kinase that acts through the c-Jun transcriptional factor to regulate gene expression during stress response and apoptosis (28). In turn, MCPs may recruit monocytes/macrophages to the tumor and CCL2 has been shown to induce angiogenesis (29). These events may further regulate the cellular composition and cytokine environment of the tumor, exerting additional effects on CSCs (30). Thus, local productions of MCPs by monocytes/macrophages and non-monocytic cells (e.g., CAF) in the tumor would likely contribute to the overall effects of MCPs before and after therapy, and be blocked by CCR2 inhibition. Although CAF do not increase MCP production upon chemotherapy treatment, previous reports show that chemotherapy increases the frequency of CAF in primary tumors and stimulates CAF to produce other cytokines that promote CSCs and chemoresistance, including IL-17A, IL-11, and IL-6 (31–33).

Notch signaling promotes self-renewal of adult stem cells [including human mammary stem cells (34)] and lineage-specific proliferation of multipotent progenitor cells [e.g., expansion of luminal progenitor cells in the mammary epithelial hierarchy (35)]. We and others have reported that Notch signaling promotes CSC phenotypes and contributes to a higher degree

of tumor malignancy (17,36,37). The post-NT activation of Notch and acquisition of CSC properties could potentially promote tumor progression and metastasis through the regulation of epithelial-to-mesenchymal transition, angiogenesis, and genes involved in invasiveness (38,39). Importantly, MCP-directed regulation of Notch may also influence hematopoietic stem/progenitor cells, as Notch activation has been shown to induce expansion of hematopoietic stem/progenitor cells (40,41). If true, this may contribute to a feed-forward loop in which MCPs produced by initial monocytes induce an expansion of HSCs and/or monocyte progenitors to produce more monocytes as sustained sources for MCPs.

Our study is based on clinical specimens from NT trials as well as experimental tumor models to simulate NT administered at an early tumor stage and to assess CSC-mediated tumor formation in an immediately post-therapy host environment. The stage of cancer and therapy simulated by these models represents the phase when CCR2 inhibition may have a beneficial effect by antagonizing the therapy-induced, monocytosis-associated cancer stemness. It is worth noting that the induction of CSC traits during NT may also impact on a subsequent metastatic event. However, metastasis is ultimately determined by multiple factors influencing cancer dormancy, molecular evolution, reprogramming upon arrival to a new site, as well as adaptation of the metastatic niche, and can occur years after the therapy-induced monocytosis through independent mechanisms (42).

CCR2 in monocytes and HSCs/HPCs mediates the mobilization of these cells from BM to inflammatory sites (43). Therefore, CCR2 inhibitors in Phase I/II clinical trials for non-cancer diseases (21,44) may act on both cancer and hematopoietic cells to efficiently block chemotherapy-induced BC stemness. Although higher levels of CCL2 in primary BCs are associated with poorer prognosis (45) and its neutralization in mice has been shown to inhibit metastasis (46), a recent study reports that cessation of CCL2 inhibition promotes BC metastasis suggesting the complication of targeting CCL2 as a monotherapy (47). Indeed, a human monoclonal antibody against CCL2 hasn’t shown antitumor activity as a single agent in metastatic castration-resistant prostate cancer patients progressing after docetaxel-based chemotherapy (48–50). These previous results highlight the need to determine the most beneficial settings for MCP-targeting therapy, which may serve to block the therapy-induced CSC phenotype when co-administered with neoadjuvant and adjuvant chemotherapies.

Supplementary Material

Refer to Web version on PubMed Central for supplementary material.

Acknowledgments

Financial support: NIH R01CA206911 (SEW&GS), R01CA218140 (SEW), R01CA163586 (SEW), P30CA23100 (UCSD Cancer Center), and P30CA33572 (City of Hope Cancer Center); the National Natural Science Foundation of China grants 81472471 (X. Ren) and 81572913 (LL); the National Key Technologies R&D Program of China grant 2015BAI12B12 (X. Ren)

This work was supported by the National Institutes of Health (NIH)/National Cancer Institute (NCI) grants R01CA206911 (SEW&GS), R01CA218140 (SEW), and R01CA163586 (SEW), the National Natural Science Foundation of China grants 81472471 (X. Ren) and 81572913 (LL), and the National Key Technologies R&D Program of China grant 2015BAI12B12 (X. Ren). Research reported in this publication included work performed in

Core facilities supported by the NIH/NCI under grant number P30CA23100 (UCSD Cancer Center) and P30CA33572 (City of Hope Cancer Center).

References

1. Thompson AM, Moulder-Thompson SL. Neoadjuvant treatment of breast cancer. Ann Oncol. 2012; 23(Suppl 10):x231–6. [PubMed: 22987968]
2. Group NM-aC. Preoperative chemotherapy for non-small-cell lung cancer: a systematic review and meta-analysis of individual participant data. Lancet. 2014; 383(9928):1561–71. [PubMed: 24576776]
3. Foxtrot Collaborative G. Feasibility of preoperative chemotherapy for locally advanced, operable colon cancer: the pilot phase of a randomised controlled trial. Lancet Oncol. 2012; 13(11):1152–60. [PubMed: 23017669]
4. Cortazar P, Geyer CE Jr. Pathological complete response in neoadjuvant treatment of breast cancer. Ann Surg Oncol. 2015; 22(5):1441–6. [PubMed: 25727556]
5. Shinde AM, Zhai J, Yu KW, Frankel P, Yim JH, Luu T, et al. Pathologic complete response rates in triple-negative, HER2-positive, and hormone receptor-positive breast cancers after anthracycline-free neoadjuvant chemotherapy with carboplatin and paclitaxel with or without trastuzumab. Breast. 2015; 24(1):18–23. [PubMed: 25467313]
6. Specht J, Gralow JR. Neoadjuvant chemotherapy for locally advanced breast cancer. Semin Radiat Oncol. 2009; 19(4):222–8. [PubMed: 19732686]
7. Coley HM. Mechanisms and strategies to overcome chemotherapy resistance in metastatic breast cancer. Cancer Treat Rev. 2008; 34(4):378–90. [PubMed: 18367336]
8. Junttila MR, de Sauvage FJ. Influence of tumour micro-environment heterogeneity on therapeutic response. Nature. 2013; 501(7467):346–54. [PubMed: 24048067]
9. Dittmer J, Leyh B. The impact of tumor stroma on drug response in breast cancer. Semin Cancer Biol. 2015; 31:3–15. [PubMed: 24912116]
10. Al-Hajj M, Wicha MS, Benito-Hernandez A, Morrison SJ, Clarke MF. Prospective identification of tumorigenic breast cancer cells. Proc Natl Acad Sci U S A. 2003; 100(7):3983–8. [PubMed: 12629218]
11. Shipitsin M, Campbell LL, Argani P, Weremowicz S, Bloushtain-Qimron N, Yao J, et al. Molecular definition of breast tumor heterogeneity. Cancer Cell. 2007; 11(3):259–73. [PubMed: 17349583]
12. Visvader JE, Lindeman GJ. Cancer stem cells in solid tumours: accumulating evidence and unresolved questions. Nat Rev Cancer. 2008; 8(10):755–68. [PubMed: 18784658]
13. Charafe-Jauffret E, Ginestier C, Iovino F, Wicinski J, Cervera N, Finetti P, et al. Breast cancer cell lines contain functional cancer stem cells with metastatic capacity and a distinct molecular signature. Cancer Res. 2009; 69(4):1302–13. [PubMed: 19190339]
14. Ginestier C, Hur MH, Charafe-Jauffret E, Monville F, Dutcher J, Brown M, et al. ALDH1 is a marker of normal and malignant human mammary stem cells and a predictor of poor clinical outcome. Cell Stem Cell. 2007; 1(5):555–67. [PubMed: 18371393]
15. Li X, Lewis MT, Huang J, Gutierrez C, Osborne CK, Wu MF, et al. Intrinsic resistance of tumorigenic breast cancer cells to chemotherapy. J Natl Cancer Inst. 2008; 100(9):672–9. [PubMed: 18445819]
16. Creighton CJ, Li X, Landis M, Dixon JM, Neumeister VM, Sjolund A, et al. Residual breast cancers after conventional therapy display mesenchymal as well as tumor-initiating features. Proc Natl Acad Sci U S A. 2009; 106(33):13820–5. [PubMed: 19666588]
17. Tsuyada A, Chow A, Wu J, Somlo G, Chu P, Loera S, et al. CCL2 mediates cross-talk between cancer cells and stromal fibroblasts that regulates breast cancer stem cells. Cancer Res. 2012; 72(11):2768–79. [PubMed: 22472119]
18. Lara-Astiaso D, Weiner A, Lorenzo-Vivas E, Zaretsky I, Jaitin DA, David E, et al. Immunogenetics. Chromatin state dynamics during blood formation. Science. 2014; 345(6199): 943–9. [PubMed: 25103404]

19. Wang SE, Narasanna A, Perez-Torres M, Xiang B, Wu FY, Yang S, et al. HER2 kinase domain mutation results in constitutive phosphorylation and activation of HER2 and EGFR and resistance to EGFR tyrosine kinase inhibitors. Cancer Cell. 2006; 10(1):25–38. [PubMed: 16843263]
20. Hu Y, Smyth GK. ELDA: extreme limiting dilution analysis for comparing depleted and enriched populations in stem cell and other assays. J Immunol Methods. 2009; 347(1–2):70–8. [PubMed: 19567251]
21. Horuk R. Chemokine receptor antagonists: overcoming developmental hurdles. Nature reviews Drug discovery. 2009; 8(1):23–33. [PubMed: 19079127]
22. Wolter S, Doerrie A, Weber A, Schneider H, Hoffmann E, von der Ohe J, et al. c-Jun controls histone modifications, NF-kappaB recruitment, and RNA polymerase II function to activate the ccl2 gene. Mol Cell Biol. 2008; 28(13):4407–23. [PubMed: 18443042]
23. Ricardo S, Vieira AF, Gerhard R, Leitao D, Pinto R, Cameselle-Teijeiro JF, et al. Breast cancer stem cell markers CD44, CD24 and ALDH1: expression distribution within intrinsic molecular subtype. J Clin Pathol. 2011; 64(11):937–46. [PubMed: 21680574]
24. Wang Y, Probin V, Zhou D. Cancer therapy-induced residual bone marrow injury-Mechanisms of induction and implication for therapy. Current cancer therapy reviews. 2006; 2(3):271–9. [PubMed: 19936034]
25. Zhu J, Emerson SG. Hematopoietic cytokines, transcription factors and lineage commitment. Oncogene. 2002; 21(21):3295–313. [PubMed: 12032771]
26. Rodier F, Coppe JP, Patil CK, Hoeijmakers WA, Munoz DP, Raza SR, et al. Persistent DNA damage signalling triggers senescence-associated inflammatory cytokine secretion. Nat Cell Biol. 2009; 11(8):973–9. [PubMed: 19597488]
27. Muhl H, Nold M, Chang JH, Frank S, Eberhardt W, Pfeilschifter J. Expression and release of chemokines associated with apoptotic cell death in human promonocytic U937 cells and peripheral blood mononuclear cells. European journal of immunology. 1999; 29(10):3225–35. [PubMed: 10540334]
28. Leppa S, Bohmann D. Diverse functions of JNK signaling and c-Jun in stress response and apoptosis. Oncogene. 1999; 18(45):6158–62. [PubMed: 10557107]
29. Stamatovic SM, Keep RF, Mostarica-Stojkovic M, Andjelkovic AV. CCL2 regulates angiogenesis via activation of Ets-1 transcription factor. J Immunol. 2006; 177(4):2651–61. [PubMed: 16888027]
30. Lu H, Clauser KR, Tam WL, Frose J, Ye X, Eaton EN, et al. A breast cancer stem cell niche supported by juxtacrine signalling from monocytes and macrophages. Nat Cell Biol. 2014; 16(11): 1105–17. [PubMed: 25266422]
31. Peiris-Pages M, Sotgia F, Lisanti MP. Chemotherapy induces the cancer-associated fibroblast phenotype, activating paracrine Hedgehog-GLI signalling in breast cancer cells. Oncotarget. 2015; 6(13):10728–45. [PubMed: 25915429]
32. Tao L, Huang G, Wang R, Pan Y, He Z, Chu X, et al. Cancer-associated fibroblasts treated with cisplatin facilitates chemoresistance of lung adenocarcinoma through IL-11/IL-11R/STAT3 signaling pathway. Scientific reports. 2016; 6:38408. [PubMed: 27922075]
33. Lotti F, Jarrar AM, Pai RK, Hitomi M, Lathia J, Mace A, et al. Chemotherapy activates cancer-associated fibroblasts to maintain colorectal cancer-initiating cells by IL-17A. J Exp Med. 2013; 210(13):2851–72. [PubMed: 24323355]
34. Dontu G, Jackson KW, McNicholas E, Kawamura MJ, Abdallah WM, Wicha MS. Role of Notch signaling in cell-fate determination of human mammary stem/progenitor cells. Breast Cancer Res. 2004; 6(6):R605–15. [PubMed: 15535842]
35. Bouras T, Pal B, Vaillant F, Harburg G, Asselin-Labat ML, Oakes SR, et al. Notch signaling regulates mammary stem cell function and luminal cell-fate commitment. Cell Stem Cell. 2008; 3(4):429–41. [PubMed: 18940734]
36. Harrison H, Farnie G, Howell SJ, Rock RE, Stylianou S, Brennan KR, et al. Regulation of breast cancer stem cell activity by signaling through the Notch4 receptor. Cancer Res. 2010; 70(2):709–18. [PubMed: 20068161]

37. Zhao D, Mo Y, Li MT, Zou SW, Cheng ZL, Sun YP, et al. NOTCH-induced aldehyde dehydrogenase 1A1 deacetylation promotes breast cancer stem cells. J Clin Invest. 2014; 124(12): 5453–65. [PubMed: 25384215]

38. Sethi N, Kang Y. Notch signalling in cancer progression and bone metastasis. Br J Cancer. 2011; 105(12):1805–10. [PubMed: 22075946]

39. Velasco-Velazquez MA, Popov VM, Lisanti MP, Pestell RG. The role of breast cancer stem cells in metastasis and therapeutic implications. Am J Pathol. 2011; 179(1):2–11. [PubMed: 21640330]

40. Karanu FN, Murdoch B, Gallacher L, Wu DM, Koremoto M, Sakano S, et al. The notch ligand jagged-1 represents a novel growth factor of human hematopoietic stem cells. J Exp Med. 2000; 192(9):1365–72. [PubMed: 11067884]

41. Varnum-Finney B, Xu L, Brashem-Stein C, Nourigat C, Flowers D, Bakkour S, et al. Pluripotent, cytokine-dependent, hematopoietic stem cells are immortalized by constitutive Notch1 signaling. Nat Med. 2000; 6(11):1278–81. [PubMed: 11062542]

42. Weigelt B, Peterse JL, van't Veer LJ. Breast cancer metastasis: markers and models. Nat Rev Cancer. 2005; 5(8):591–602. [PubMed: 16056258]

43. Si Y, Tsou CL, Croft K, Charo IF. CCR2 mediates hematopoietic stem and progenitor cell trafficking to sites of inflammation in mice. J Clin Invest. 2010; 120(4):1192–203. [PubMed: 20234092]

44. Sullivan T, Miao Z, Dairaghi DJ, Krasinski A, Wang Y, Zhao BN, et al. CCR2 antagonist CCX140-B provides renal and glycemic benefits in diabetic transgenic human CCR2 knockin mice. American journal of physiology Renal physiology. 2013; 305(9):F1288–97. [PubMed: 23986513]

45. Ueno T, Toi M, Saji H, Muta M, Bando H, Kuroi K, et al. Significance of macrophage chemoattractant protein-1 in macrophage recruitment, angiogenesis, and survival in human breast cancer. Clin Cancer Res. 2000; 6(8):3282–9. [PubMed: 10955814]

46. Qian BZ, Li J, Zhang H, Kitamura T, Zhang J, Campion LR, et al. CCL2 recruits inflammatory monocytes to facilitate breast-tumour metastasis. Nature. 2011; 475(7355):222–5. [PubMed: 21654748]

47. Bonapace L, Coissieux MM, Wyckoff J, Mertz KD, Varga Z, Junt T, et al. Cessation of CCL2 inhibition accelerates breast cancer metastasis by promoting angiogenesis. Nature. 2014; 515(7525):130–3. [PubMed: 25337873]

48. Crusz SM, Balkwill FR. Inflammation and cancer: advances and new agents. Nat Rev Clin Oncol. 2015; 12(10):584–96. [PubMed: 26122183]

49. Sandhu SK, Papadopoulos K, Fong PC, Patnaik A, Messiou C, Olmos D, et al. A first-in-human, first-in-class, phase I study of carlumab (CNTO 888), a human monoclonal antibody against CC-chemokine ligand 2 in patients with solid tumors. Cancer Chemother Pharmacol. 2013; 71(4): 1041–50. [PubMed: 23385782]

50. Pienta KJ, Machiels JP, Schrijvers D, Alekseev B, Shkolnik M, Crabb SJ, et al. Phase 2 study of carlumab (CNTO 888), a human monoclonal antibody against CC-chemokine ligand 2 (CCL2), in metastatic castration-resistant prostate cancer. Invest New Drugs. 2013; 31(3):760–8. [PubMed: 22907596]

Translational Relevance

Preoperative or neoadjuvant therapy is increasingly administered to patients who are candidates for breast preservation and/or present with locally advanced or inflammatory breast cancer. However, some patients poorly respond to the treatment or relapse after neoadjuvant therapy. Our study using patient blood samples and experimental cell and mouse models shows that cytotoxic chemotherapy induces circulating monocyte-derived chemokines, which stimulate cancer stem-like cells (CSCs) to potentially promote tumor relapse. Therefore, effective anticancer therapies need to block the concurrent CSC-stimulating effect to achieve better short-term and long-term outcomes. Using pre-clinical tumor models, we show that pharmacological inhibition of CCR2 can serve as a potential co-treatment during conventional chemotherapy by targeting therapy-induced cancer stemness. In primary breast tumors, higher levels of CCR2 in tumor cells are associated with lack of a pathologic complete response to neoadjuvant therapy.

Statement of Significance

We find that cytotoxic chemotherapy induces circulating monocyte-derived chemokines, which stimulate the cancer stem-like cell phenotype to potentially promote tumor resistance and relapse. Our study suggests pharmacological inhibition of CCR2 as a potential co-treatment during conventional chemotherapy to target therapy-induced cancer stemness, especially in tumors with high levels of CCR2.

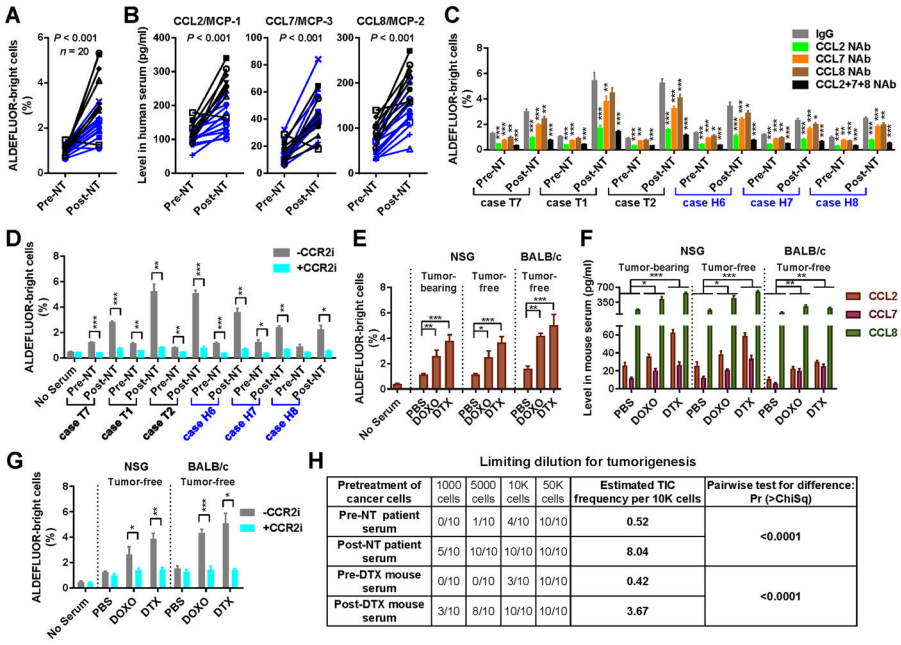

Pretreatment of cancer cells	1000 cells	5000 cells	10K cells	50K cells	Estimated TIC frequency per 10K cells	Pairwise test for difference: Pr (>ChiSq)
Pre-NT patient serum	0/10	1/10	4/10	10/10	0.52	<0.0001
Post-NT patient serum	5/10	10/10	10/10	10/10	8.04	
Pre-DTX mouse serum	0/10	0/10	3/10	10/10	0.42	<0.0001
Post-DTX mouse serum	3/10	8/10	10/10	10/10	3.67	

Figure 1. Post-chemotherapy sera from BC patients and mice stimulate a CSC phenotype through elevated MCP levels

(**A**) Twenty pairs of pre- and post-NT sera from TNBC (*n*=8; black) or HER2^{+} BC (*n*=12; blue) patients were analyzed for the activity to stimulate the ALDEFLUOR^{bright} population of BC cells. MDA-MB-231 cells were cultured for 48 h in base medium supplemented with 10% human serum before ALDEFLUOR assays by flow cytometry. Wilcoxon test was performed. (**B**) ELISA to determine the levels of human CCL2/7/8 in the 20 pairs of sera. Wilcoxon tests were performed. (**C**) ALDEFLUOR assays using 6 pairs of sera (3 cases for each BC subtype) were performed as in **A** except that CCL2/7/8 neutralizing antibodies (NAb; 30 ng/ml; alone or all 3 combined) or control IgG were added during serum treatment. (**D**) ALDEFLUOR assays of MDA-MB-231 cells treated with patient sera in the presence of a CCR2 inhibitor (MK-0812; 600 nM) or vehicle. (**E**) NSG mice with or without MDA-MB-231 xenograft tumors and tumor-free BALB/c mice received 3 weekly injections with doxorubicin (DOXO; 4 mg/kg) or docetaxel (DTX; 25 mg/kg) (*n*=3). Six days later, serum was collected to treat MDA-MB-231 cells for ALDEFLUOR assays as in **A**. (**F**) ELISA to determine the serum levels of mouse CCL2/7/8. (**G**) ALDEFLUOR assays of MDA-MB-231 cells treated with mouse sera in the presence of the CCR2 inhibitor MK-0812 or vehicle. (**H**) Sera from chemotherapy-treated patients and mice induce tumorigenicity. MDA-MB-231 cells pre-treated with human (case T1) or mouse (tumor-free BALB/c) sera for 48 h were injected into the mammary fat pad of NSG mice (*n*=10) at the indicated numbers. Tumor incidence after 4 weeks was shown. The estimated TIC frequency was estimated by ELDA. **P*<0.05, ***P*<0.01, ****P*<0.001 (compared to the corresponding IgG group in **C** or as indicated).

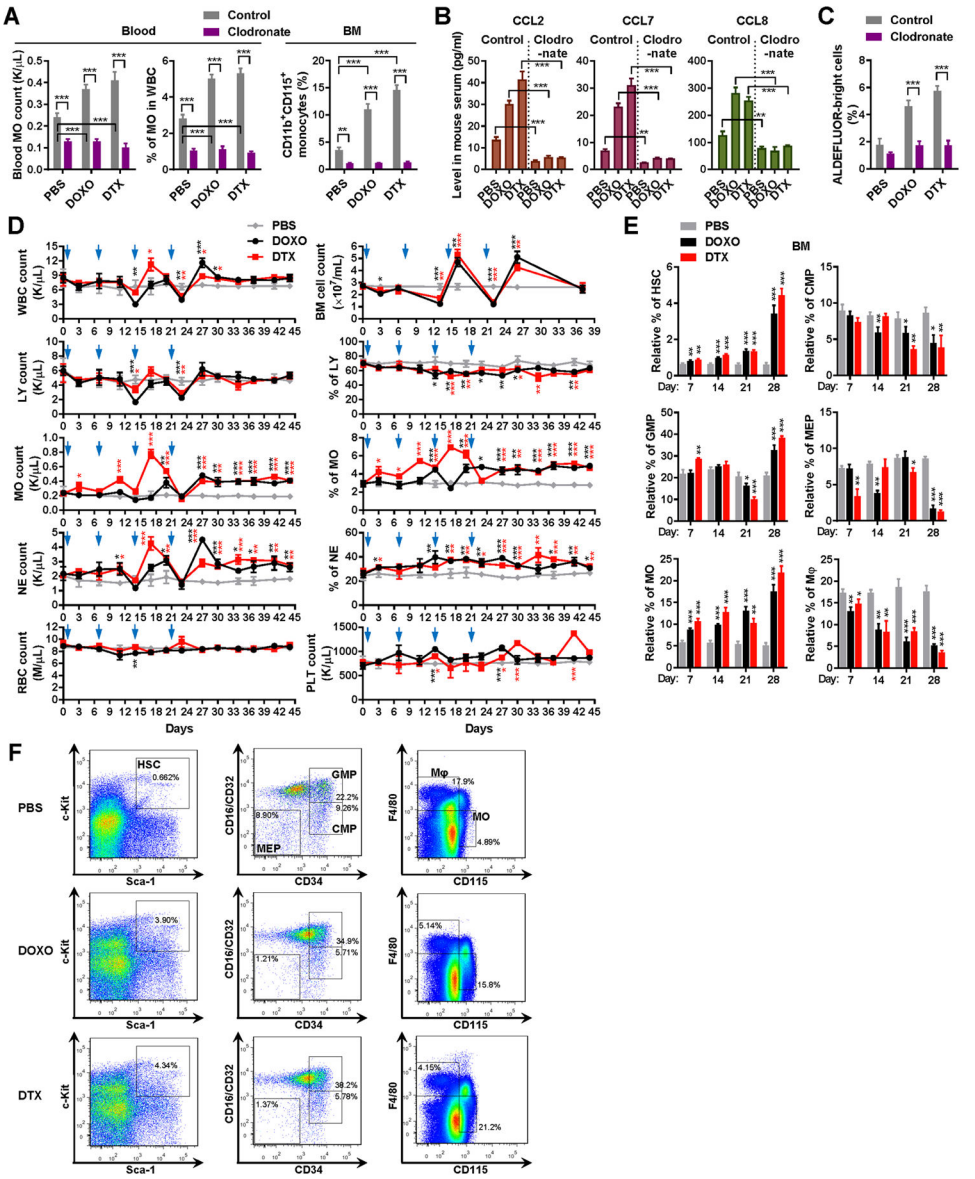

Figure 2. Chemotherapy-induced monocytosis is responsible for the elevation of circulating MCPs

(**A**) Clodronate liposomes or control were injected into BALB/c mice through the tail vein every 2 days starting at 2 days prior to the first chemotherapy treatment (n=3). At day 6 after 3 weeks of chemotherapy, the number and percentage (out of total white blood cells) of monocytes were analyzed by a complete blood count (left). The $CD11b^{+}CD115^{+}$ monocyte population in the BM was analyzed by flow cytometry (right). (**B**) ELISA to determine the serum levels of mouse CCL2/7/8 (n=3). (**C**) ALDEFLUOR assays of MDA-MB-231 cells treated with indicated mouse sera (n=3). (**D**) Chemotherapy induces expansion of monocytes in the rebound phase. BALB/c mice received 4 times of treatment with DOXO or DTX, or PBS on days 1, 7, 14, and 21 (blue arrowheads). At each indicated time point, complete blood count was conducted to determine the numbers and percentages of various cell populations (n=3). Total BM cell count was also shown. WBC: white blood cells; LY:

lymphocytes; MO: monocytes; NE: neutrophils; RBC: red blood cells; PLT: platelets. On days 7 and 14, blood was collected before treatment. (**E**) BM cells were collected at the indicated time from C57BL/6 mice that have received 1–4 times of treatment with DOXO or DTX, or PBS (treatments given on days 1, 7, 14, and 21). Flow cytometry was performed to determine the population of indicated cell types (n=3). HSC: hematopoietic stem cells; CMP: common myeloid progenitors; GMP: granulocyte-monocyte progenitors; MEP: megakaryocyte-erythrocyte progenitors. (**F**) Representative flow cytometry plots on day 28 from all three groups in **E**. *P<0.05, **P<0.01, ***P<0.001 (compared to the corresponding PBS group in **D** & **E** or as indicated).

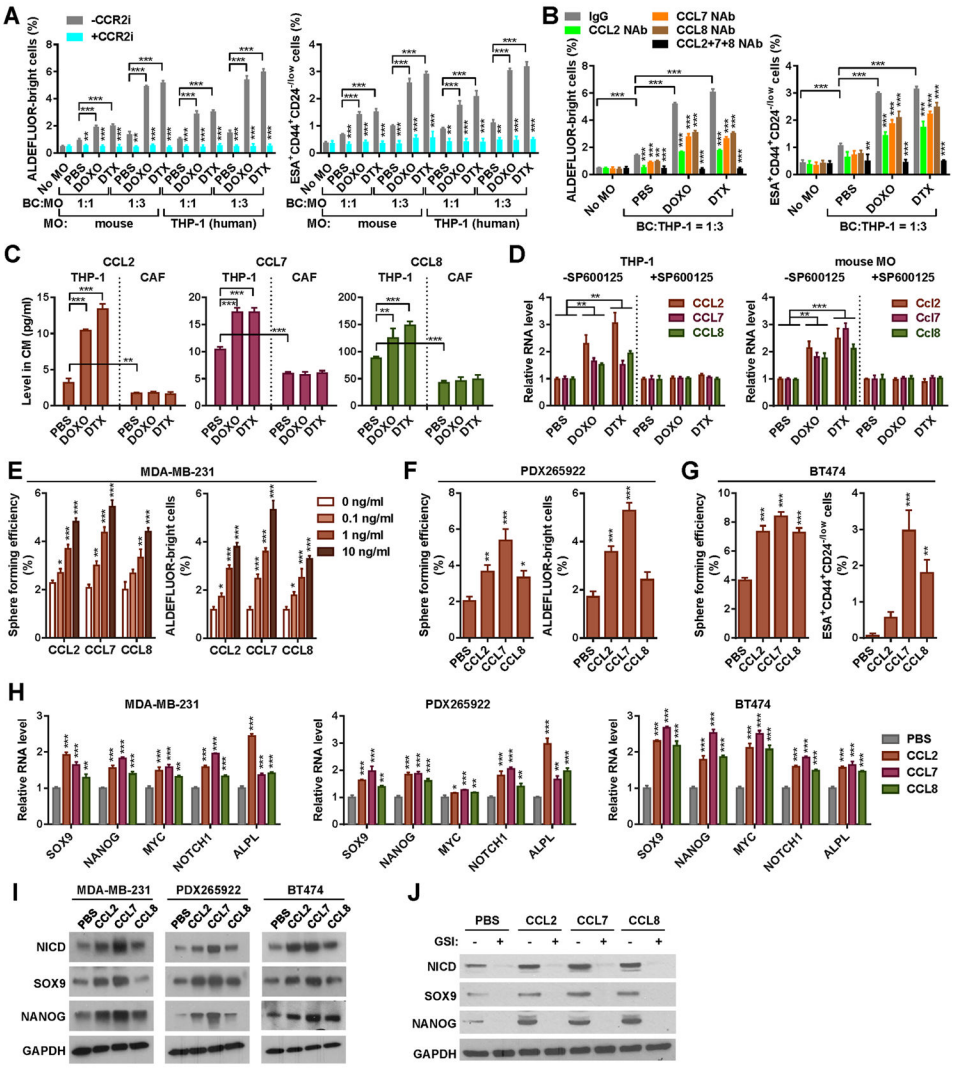

Figure 3. Chemotherapy induces monocyte expression of MCPs, which promote the stemness-associated properties by inducing Notch

(**A** & **B**) Co-cultures were set up using MDA-MB-231 or BT474 BC cells with monocytes isolated from C57BL/6 mice treated with DOXO, DTX, or PBS, or with DOXO/DTX/PBS-pretreated THP-1 cells, in the presence or absence of the CCR2 inhibitor MK-0812 (**A**) or CCL2/7/8 NAb (**B**) as described in Materials and Methods. BC cells and monocytes were seeded at a ratio of 1:1 or 1:3. ALDEFLUOR assays (for MDA-MB-231) and ESA $^{+}$CD44^{+}CD24$^{-/low}$ flow cytometry (for BT474) were performed using BC cells harvested after 48 h of co-culture. (**C**) MCP secretion by THP-1 and CAF was determined by ELISA of the conditioned media (CM) of 10^5 THP-1 cells or cancer-activated CAF (pre-treated with the CM from PDX265922 cancer cells) that had been treated with DOXO (125 nM), DTX (4 nM), or PBS for 48 h. (**D**) THP-1 cells under DOXO/DTX/PBS treatment and mouse monocytes isolated as in **A** were cultured in the presence or absence of a JNK inhibitor SP600125 (1 μM) for 48 h and analyzed by quantitative RT-PCR using GAPDH/Gapdh for normalization. (**E**) MDA-MB-231 cells were treated with CCL2/7/8 at the indicated concentrations for 48 h and analyzed by sphere formation assay or ALDEFLUOR assay. (**F**)

PDX265922 cells derived from a primary TNBC were treated with CCL2/7/8 (1 ng/ml) or PBS for 48 h and analyzed by sphere formation assay or ALDEFLUOR assay. (**G**) CCL2/7/8-treated BT474 cells were analyzed by sphere formation assay or flow cytometry for the $ESA^{+}CD44^{+}CD24^{-/low}$ population. (**H**) Indicated BC cells were treated with CCL2/7/8 (1 ng/ml) or PBS for 24 h and analyzed by quantitative RT-PCR for indicated stemness-related genes. Data are normalized to GAPDH and compared to the PBS group. (**I**) Western blot analysis showing stemness-associated gene expression in BC cells treated with CCL2/7/8 or PBS for 24 h. (**J**) Western blot analysis of MDA-MB-231 cells treated with CCL2/7/8 or PBS in the presence or absence of a γ-secretase inhibitor (GSI) RO4929097 (10 μM). *$P<0.05$, **$P<0.01$, ***$P<0.001$ (compared to the control group in the first column of each group or as indicated).

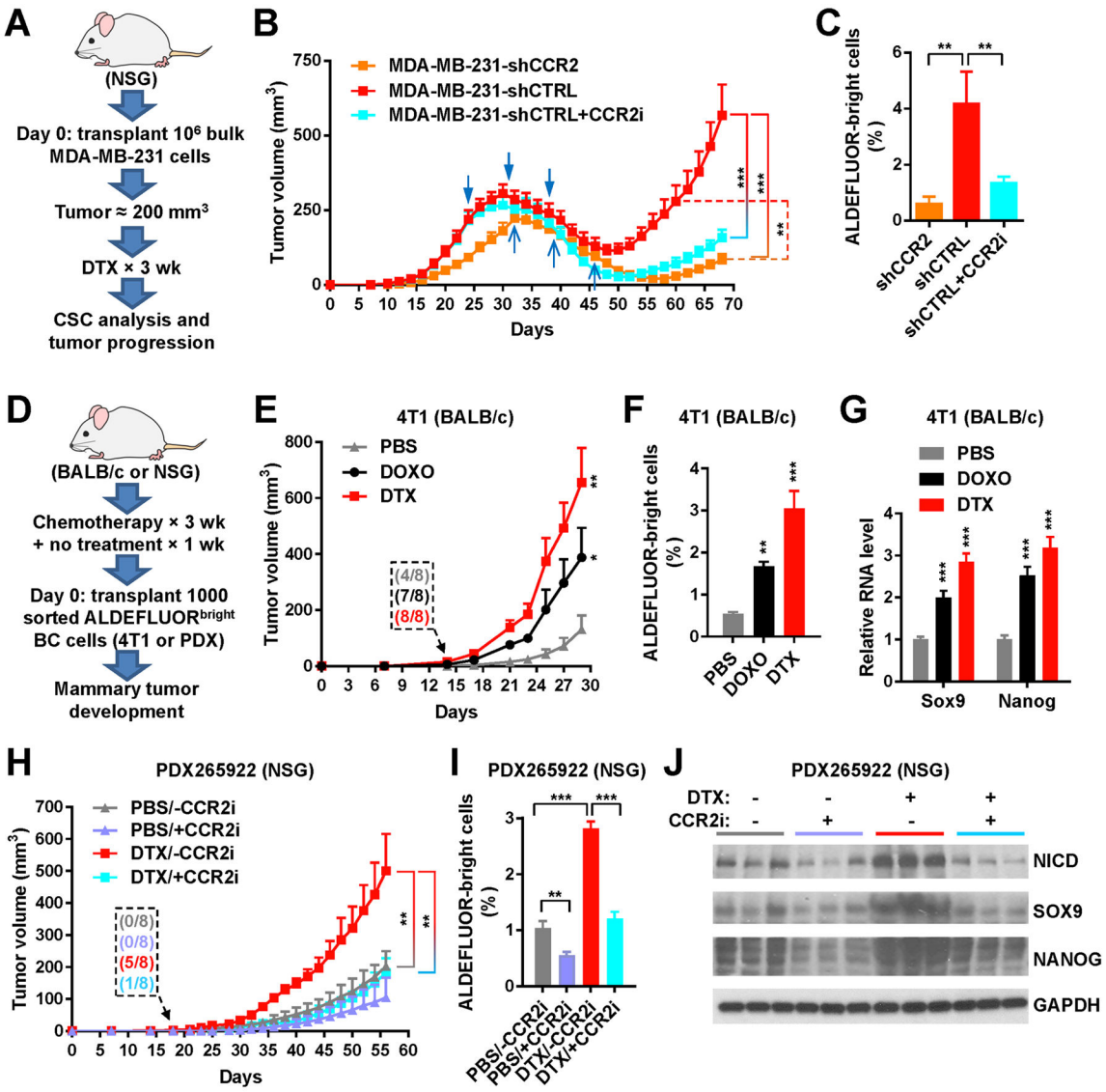

Figure 4. Chemotherapy promotes CSC properties *in vivo* through MCP-CCR2 signaling

(**A**) Schema of the mouse model used to examine if CCR2 intervention suppresses post-chemotherapy tumor progression. One million of MDA-MB-231 cells with stable knockdown of CCR2 (shCCR2) or those expressing control shRNA (shCTRL) were injected into the #4 mammary fat pad of NSG mice. When tumor size reached ~250 mm^3, mice were treated with DTX for 3 weeks, and then left free of chemotherapy until the end of experiment. One group with MDA-MB-231-shCTRL tumors also received the CCR2 inhibitor MK-0812 starting with the chemotherapy and continuing for a total of 30 days, whereas the other two groups received the vehicle. (**B**) Tumor onset and volume (n=8). The two groups with MDA-MB-231-shCTRL tumors received 3 times of treatment with DTX on days 24, 31, and 38 (blue arrowheads); the group with MDA-MB-231-shCCR2 tumors received DTX on days 32, 39, and 46 (blue arrows). (**C**) ALDEFLUOR assay of dissociated MDA-MB-231 tumor cells. (**D**) Schema of the mouse models used to examine if chemotherapy prior to BC cell engraftment enhances tumor formation. BALB/c and NSG

mice were treated with DOXO, DTX, or PBS for 3 weeks and then left free of chemotherapy for 1 week, before 1000 FACS-isolated ALDEFLUOR^{bright} 4T1 or PDX265922 cells were injected into the #4 mammary fat pad to assess tumor development. (**E**) Tumor onset and volume for the 4T1 model in BALB/c mice (n=8). Inset shows numbers of mice with palpable tumors on day 14. (**F**) ALDEFLUOR assay of dissociated 4T1 tumor cells. (**G**) Relative RNA levels of indicated genes (normalized to Gapdh) in 4T1 tumor tissue determined by quantitative RT-PCR assay. (**H**) Tumor onset and volume for the PDX265922 model in NSG mice (n=8). CCR2 inhibitor MK-0812 or vehicle was orally administered at 30 mg/kg twice a day starting with the chemotherapy and continuing for 30 days after BC cell engraftment. Inset shows numbers of mice with palpable tumors on day 18. (**I**) ALDEFLUOR assay of dissociated PDX265922 tumor cells. (**J**) Western analysis showing indicated protein levels in PDX265922 tumor tissue. *P<0.05, **P<0.01, ***P<0.001 (compared to the corresponding PBS group in **E–G** or as indicated).

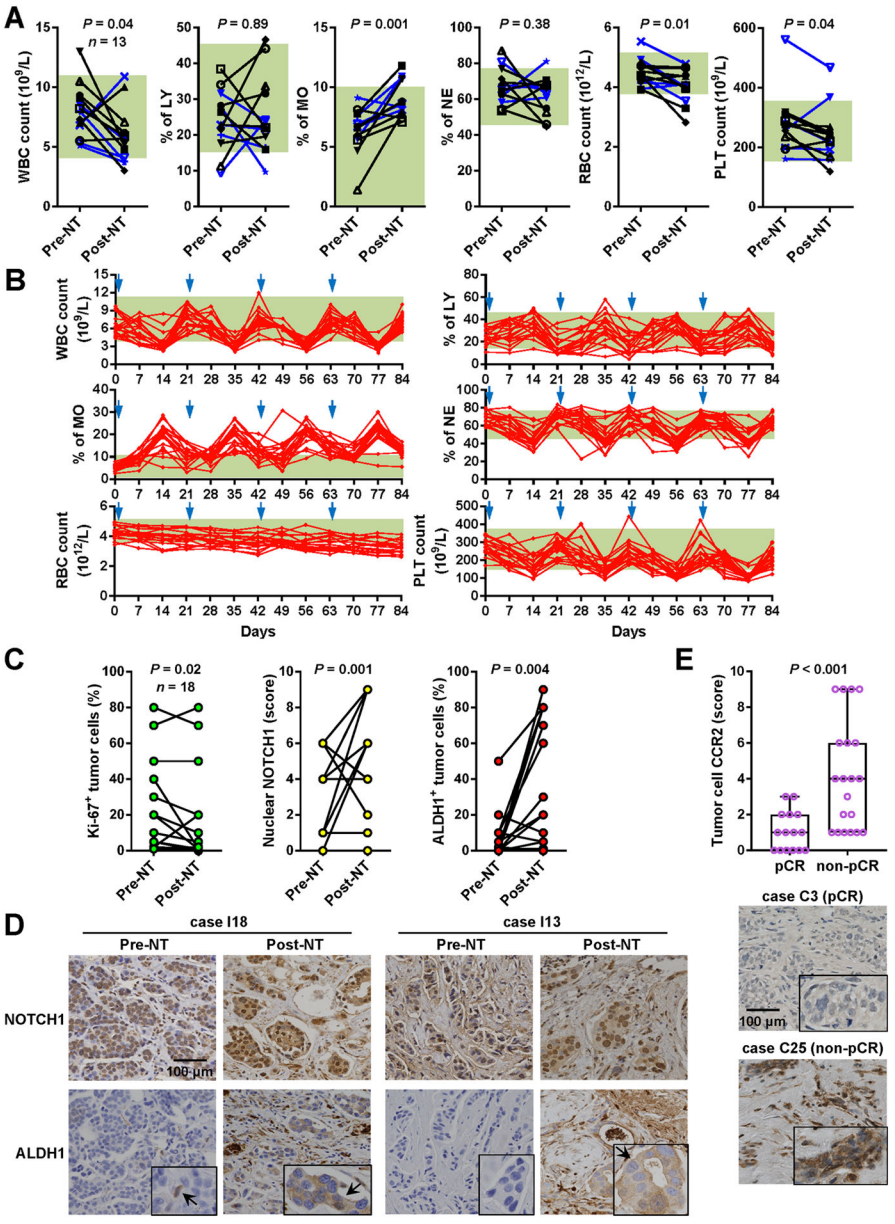

Figure 5. Chemotherapy-induced monocytosis and tumor expression of NOTCH1, ALDH1, and CCR2 in BC patients

(**A**) Complete blood count showing changes of various cell populations upon NT in a total of 13 patients including 8 cases of TNBC (black) and 5 cases of $HER2^+$ BC (blue) that were treated at the City of Hope National Medical Center. The green boxes in the background indicate normal ranges. Wilcoxon tests were performed. (**B**) Complete blood count showing the dynamics of various cell populations during 4 cycles of NT in 19 BC patients treated at the Tianjin Medical University Cancer Institute and Hospital. The start of each cycle is indicated by a blue arrowhead. The green boxes in the background indicate normal ranges. (**C**) Eighteen pairs of pre- and post-NT breast tumors from the City of Hope patients were analyzed by immunohistochemistry (IHC) to show the percentages of tumor cells positive for Ki-67 or ALDH1, as well as the staining scores for nuclear NOTCH1 in tumor cells.

Wilcoxon tests were performed. (**D**) Representative IHC images from two cases. (**E**) Pre-NT breast tumors were analyzed by IHC for the expression of CCR2 in tumor cells. Tumors with pCR (n=15) were compared to those with non-pCR (n=20). Mann–Whitney test was performed. Representative IHC images are shown.

Table 1

Serum CSC-stimulating activity and MCP levels in stratified patients.*

Stratification by response to NT (total *n* = 20)				
		pCR (*n* = 9)	**non-pCR (*n* = 11)**	**pCR vs. non-pCR *P* value**
ALDEFLUOR$^+$ (% of MDA-MB-231)	Pre-NT	1.02 ± 0.19	1.03 ± 0.23	>0.99
	Post-NT	3.52 ± 1.36	1.96 ± 0.61	**0.004**
	Pre vs. Post *P* value	**0.004**	**0.005**	
ESA$^+$CD44$^+$CD24$^{-/low}$ (% of BT474)	Pre-NT	0.66 ± 0.20	0.68 ± 0.27	0.55
	Post-NT	2.67 ± 0.68	2.01 ± 0.77	0.05
	Pre vs. Post *P* value	**0.004**	**0.002**	
CCL2/MCP-1 (pg/ml)	Pre-NT	109.1 ± 24.6	116.1 ± 34.1	0.52
	Post-NT	222.2 ± 83.8	177.8 ± 54.8	0.23
	Pre vs. Post *P* value	**0.004**	**0.003**	
CCL7/MCP-3 (pg/ml)	Pre-NT	15.6 ± 8.1	14.0 ± 7.2	0.71
	Post-NT	48.2 ± 18.1	37.9 ± 13.1	0.08
	Pre vs. Post *P* value	**0.004**	**0.002**	
CCL8/MCP-2 (pg/ml)	Pre-NT	74.7 ± 29.7	73.5 ± 34.5	0.72
	Post-NT	185.9 ± 59.0	136.8 ± 42.8	0.10
	Pre vs. Post *P* value	**0.004**	**<0.001**	
Stratification by HER2 status (total *n* = 20)				
		TN (*n* = 8)	HER2$^+$ (*n* = 12)	TN vs. HER2$^+$ *P* value
ALDEFLUOR$^+$ (% of MDA-MB-231)	Pre-NT	1.06 ± 0.23	1.00 ± 0.21	0.68
	Post-NT	3.65 ± 1.42	2.00 ± 0.57	**0.005**
	Pre vs. Post *P* value	**0.02**	**<0.001**	
ESA$^+$CD44$^+$CD24$^{-/low}$ (% of BT474)	Pre-NT	0.63 ± 0.30	0.70 ± 0.18	0.68
	Post-NT	2.15 ± 0.89	2.41 ± 0.74	0.68
	Pre vs. Post *P* value	**0.02**	**<0.001**	
CCL2/MCP-1 (pg/ml)	Pre-NT	128.8 ± 29.2	102.4 ± 26.0	**0.05**
	Post-NT	262.1 ± 53.6	154.9 ± 43.3	**<0.001**
	Pre vs. Post *P* value	**0.02**	**<0.001**	
CCL7/MCP-3 (pg/ml)	Pre-NT	16.4 ± 7.3	13.7 ± 7.6	0.34
	Post-NT	37.7 ± 16.3	45.7 ± 15.6	0.25
	Pre vs. Post *P* value	**0.02**	**<0.001**	
CCL8/MCP-2 (pg/ml)	Pre-NT	98.5 ± 27.3	57.7 ± 22.8	**0.002**
	Post-NT	207.5 ± 39.0	126.5 ± 38.1	**<0.001**
	Pre vs. Post *P* value	**0.008**	**<0.001**	

[*] The 20 pairs of pre- and post-NT sera in Figure 1A–B and Supplemental Figure 1A were stratified by BC's response to NT (pCR vs. non-pCR) or HER2 status (TN vs. $HER2^+$) before summarized for the activity to stimulate CSC populations and for levels of CCL2/7/8 in the format of mean ± standard deviation. Wilcoxon test was used to calculate the Pre vs. Post *P* value, whereas Mann–Whitney test was used for pCR vs. non-pCR *P* value and TN vs. $HER2^+$ *P* value.